TOWARDS AUTOMATIC AVALANCHE DETECTION AND CHARACTERIZATION USING SEISMIC AND INFRASOUND ARRAY DATA

Christine Seupel*[1], Patrick Düggelin[1], Andri Simeon[1], Cristina Pérez-Guillén[1], Andreas Fichtner[2], Alec van Herwijnen[1]

[1] *WSL Institute for Snow and Avalanche Research SLF, Davos, Switzerland*
[2] *Department of Earth and Planetary Sciences, ETH Zürich, Institute of Geophysics, Zürich, Switzerland*

ABSTRACT: Reliable avalanche detection and localization are essential for effective hazard mitigation. They support avalanche forecasting, risk management, and the development of new, data-driven forecasting tools. Both seismic and infrasound sensors can be used to record avalanche signals. Generated by different parts of the avalanche flow, these signals contain complementary information. When deployed as arrays, seismic and infrasound sensors enable advanced signal processing to estimate source parameters, including apparent velocity and backazimuth, which can be used to locate avalanches. Although both types of systems are well suited for avalanche detection and localization, each possesses specific strengths and limitations that can be exploited in a complementary manner. To investigate this potential, we installed a co-located seismo-acoustic array of five seismic and five infrasound sensors in the Dischma Valley near Davos, Switzerland. We have recorded continuous data since the 2020-2021 winter season. While infrasound array processing yields stable and coherent source parameters even when signal amplitudes are close to the noise level, beamforming results from seismic data are more variable but still robust. In addition, cross-correlation between co-located seismic and infrasound sensors reveals distinct patterns of seismo-acoustic coupling that reflect differences in avalanche types. Based on these findings, we are developing a combined seismo–acoustic detection framework that exploits array-derived source parameters to automatically detect avalanches and provide additional information on avalanche type and flow regime. Specifically, the framework identifies candidate avalanche signals using threshold-based rules applied to source parameters, signal amplitudes, and durations, while cross-correlations between seismic and infrasound signals are used to estimate the avalanche type. We evaluate the detection algorithm using a dataset of avalanche signals recorded over five winter seasons. Preliminary results are promising, indicating that the combination of seismic and infrasound data improves detection robustness, while also enabling basic avalanche characterization.

KEYWORDS: Avalanche Detection, Seismic, Infrasound, Array Processing, Instrumentation and Remote Sensing

1. INTRODUCTION

Accurate avalanche detection and localization are crucial for effective hazard mitigation in alpine regions. Seismic and infrasound arrays are well-established tools to monitor avalanche activity and locate avalanche events in large areas, regardless of weather conditions or visibility (Heck et al. 2018; Mayer et al. 2020; Johnson et al. 2021; Belli et al. 2025). Seismic signals are generated mainly by the flowing avalanche interacting with the ground (Vilajosana et al. 2007; Pérez-Guillén et al. 2016), while infrasound generation is driven mainly by the suspension layer (Marchetti, van Herwijnen, et al. 2020; Sovilla et al. 2025). Consequently, these two sensor types provide complementary information (Kogelnig et al. 2011; Seupel et al. 2026). As a result, using each system alone for avalanche detection comes with its own limitations.

To date, several infrasound array based detection systems have been developed (Marchetti, Ripepe, et al. 2015; Belli et al. 2025), some of them are in operational use (Steinkogler et al. 2016; Chen et al. 2024). However, infrasound-only approaches tend to miss wet-snow or mixed avalanches, as they exhibit lower detection rates than for dry-snow avalanches (Mayer et al. 2020). In contrast, seismic sensors have the potential to detect avalanches independently of their flow regime. However, no operational avalanche detection system based solely on seismic arrays is currently in use, as seismic signals are more complex and prone to a wider variety of noise sources. Beyond avalanche detection, the combination of seismic and infrasound observations can also be used to characterize avalanches, as the relationship between the two signal types varies between different avalanche flow types (Seupel et al. 2026).

These findings motivated us to develop the seismo-acoustic avalanche detection and characterization workflow presented here. The workflow applies a physics- and threshold-based approach, designed to facilitate its transfer to other locations. By inte-

* *Corresponding author address:*
Christine Seupel
WSL Institute for Snow and Avalanche Research SLF
Flüelastrasse 11, 7260 Davos Dorf, Switzerland
tel.: +41 81 4170 358
email: christine.seupel@slf.ch

grating seismic and infrasound data, the proposed framework aims to combine the robust detection performance of established infrasound-based detection methods with additional information from seismic observations. Incorporating seismic observations is particularly useful for detecting small wet-snow avalanches and for avalanche classification. Furthermore, we highlight that this instrumental setup still enables the use of already established detection workflows, whether array- or single-sensor-based. Thus, it provides the benefits of combining seismic and infrasound array recordings while retaining the ability to use existing detection approaches.

2. FIELDSITE AND DATASET

2.1. Fieldsite and Instrumentation

We installed a seismo-acoustic array at our fieldsite in the Dischma valley above Davos, Switzerland, for six winter seasons starting in 2020/2021 (Figure 1). The array consists of five co-located seismometers and infrasound sensors, deployed in a triangular geometry with an aperture of 110 m (Figure 1b). The seismic array comprised one 3-component Lennartz LE-3Dlite and four 1-component LE-1DV seismometers, while the infrasound array comprised five Prs0025a pressure sensors from ITEM s.r.l. Data were recorded continuously with a sampling frequency of 200 Hz. To improve the signal-to-noise ratio, we buried the seismometers and installed the infrasound sensors in partially buried tubes topped with a lid that allows air circulation (Figure 1c). Avalanche activity was visually monitored using 12 automatic cameras at three locations around the fieldsite, which recorded images every 10–30 min. Beginning in winter 2021/2022, a Doppler avalanche radar was also deployed facing one main avalanche path to provide independent avalanche release times and validation data (Figure 1a).

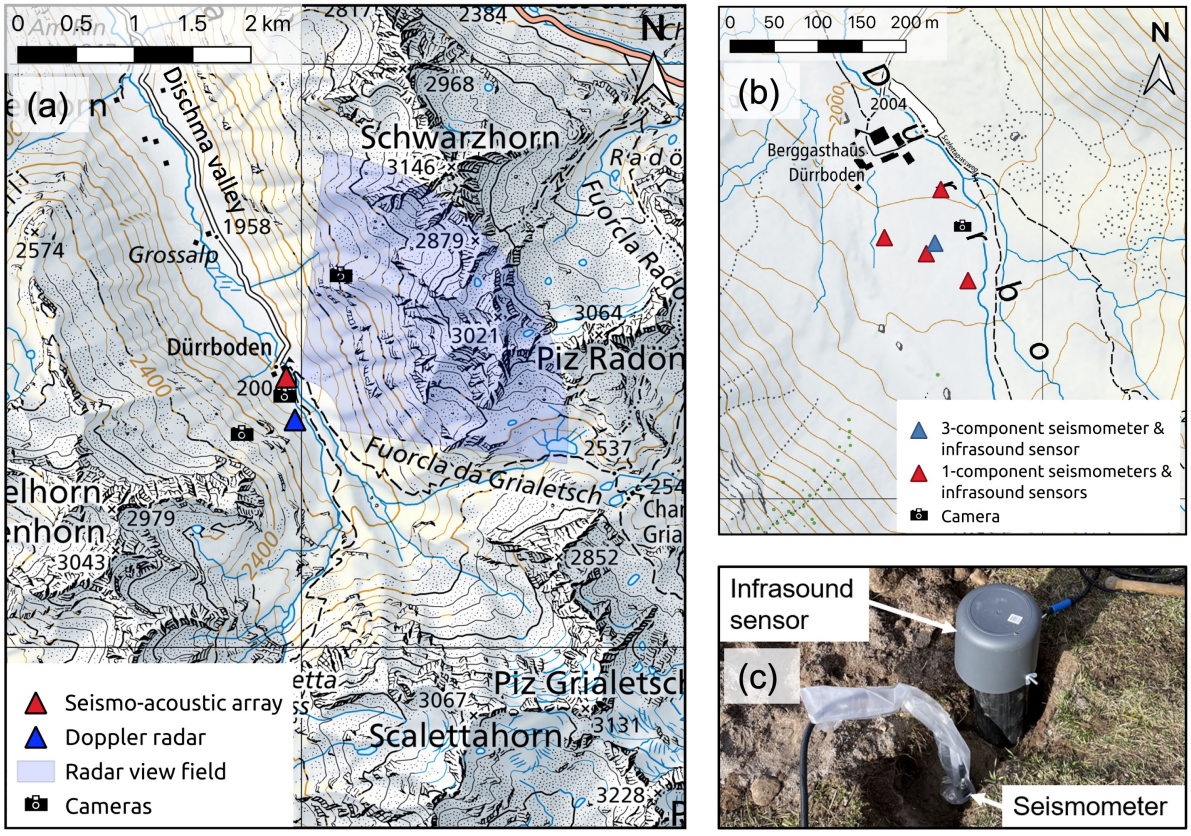


Figure 1: (a) Location of the seismo-acoustic array, Doppler radar, and camera positions at our fieldsite in the Dischma valley. The blue colored area marks the slope regions within the radar's field of view. (b) Location of the different sensors of the seismo-acoustic array at Dürrboden. (c) Seismometer and an infrasound sensor installed in the field (map source: Federal Office of Topography), (reproduced from (Seupel et al. 2026)).

2.2. Dataset

To obtain an avalanche catalog for workflow development, we labeled data from five winter seasons using a procedure similar to that of Simeon et al. (2025). First, radar data and automatic camera images were used to identify periods of avalanche activity. Within these periods, all potential events (e.g. avalanches, earthquakes, airplanes, and other noise) were visually identified in the seismic and infrasound data. Then three experts independently classified each event for each array (seismic and infrasound) as no avalanche (0), maybe avalanche (0.5), or avalanche (1). The resulting labels were summed to obtain an avalanche score ranging from 0 (no expert thought the signal was an avalanche in seismic or infrasound) to 6 (all experts were certain the signal was from an avalanche in seismic and infrasound data). Signal duration was manually picked by an expert from the time series of a single seismometer and infrasound sensor. Events with a score ≥ 3.5 were classified as avalanches for workflow development, resulting in 134 avalanches and 1,654 noise events throughout the five winter seasons of 2020/2021 - 2024/2025. Figure 2 shows an example of the seismic and infrasound signal generated by a wet-snow avalanche released at our fieldsite, further examples are presented in Seupel et al. (2026).

In addition, we classified each avalanche event as a dry- or wet-snow avalanche to determine whether distinguishing these avalanche types is possible from seismic and infrasound recordings alone. However, visual classification using camera images is often insufficient, and regular measurements of snow liquid water content could not be acquired across all winter seasons. We therefore conducted SNOWPACK simulations (Lehning et al. 2002; Bartelt and Lehning 2002) to evalute the state of the snow-pack (dry or wet). Specifically, we simulated the flat-field snow cover driven at a 3-h temporal resolution using real-time meteorological data from the automatic weather station Bärentälli in Davos (2558 m a.s.l., $\sim$8 km from the release areas at similar elevation). To evaluate avalanche types, each event was categorized using the simulated mean liquid water content (LWC) into three classes: dry (LWC $= 0$), mixed ($0 <$ LWC ≤ 1.5), and wet (LWC > 1.5). The mixed class should account for transitional periods, e.g., when aspect-dependent warming induces wet avalanches on water-saturated south-facing slopes, while cold north-facing slopes remain dry. This results in 54 dry-snow avalanches, 66 wet-snow avalanches, and 14 avalanches in the mixed class.

3. WORKFLOW

Our detection and characterization workflow is inspired by existing threshold-based infrasound array approaches, (e.g. Belli et al. 2025), which combine array-processing techniques, such as beamforming and cross-correlation, with time-series and frequency-domain features. The array processing techniques used in our workflow are described below. First, cross-correlations quantify the similarity between two signals and provide a correlation coefficient (0–1) and a time lag. A coefficient close to one indicates similar signals, while a time lag close to zero indicates simultaneous signal arrival at the sensors. Cross-correlations can be calcu-

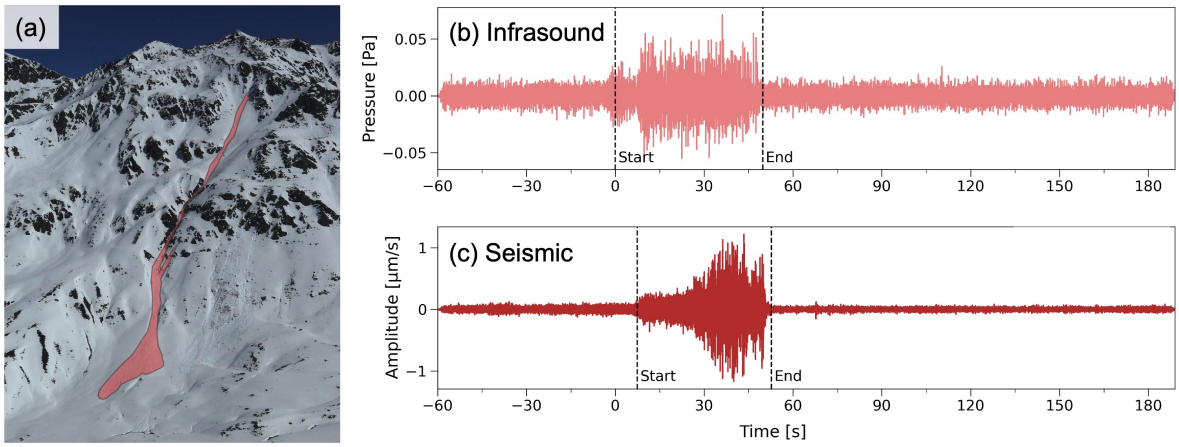


Figure 2: Data from a wet-snow avalanche released at our fieldsite: (a) Image taken by an automatic camera one day after the avalanche released. The avalanche outline is shown in red. (b) Waveform of the central infrasound sensor. (c) Waveform of the vertical component of the central seismometer (reproduced from (Seupel et al. 2026)).

lated either between sensors of the same type, which is used for event detection in our workflow, or between co-located seismic and infrasound sensors. The latter provides information on seismo-acoustic coupling and source processes (Seupel et al. 2026) and is therefore used to characterize avalanches. Second, beamforming uses the different arrival times of a plane wavefront arriving at all sensors to determine the backazimuth, the angle from which the signal is coming, and the apparent velocity, which is the wavefront velocity (Rost and Thomas 2002). For our detection workflow, we adapted the fast beamforming algorithm of Schippkus (2025).

We developed the detection and classification workflow using data from the first three winter seasons (2020/2021–2022/2023), which contained 89 avalanches (31 dry-snow, 52 wet-snow, and 6 in the mixed class). The remaining two winter seasons (2023/2024–2024/2025) were reserved as a test set.

3.1. Avalanche Detection

The detection workflow is written in Python and is currently under development. Here, we outline its basic workflow, which relies on a two-step approach that combines seismic and infrasound array processing (Figure 3). Before entering the detection framework, we preprocessed the raw data. As most of the avalanche energy at our study site is concentrated at low frequencies, seismic and infrasound data were bandpass-filtered between 2 and 10 Hz. Furthermore, for seismic data, a 5–7 Hz bandstop filter was applied to suppress a local persistent noise band.

The first part of the detection framework, the event detector, is designed to identify seismo-acoustic events from continuous seismic and infrasound data. It is optimized for high sensitivity (recall) so that, ideally, all potential avalanche signals are captured, even at the cost of generating many non-avalanche noise events. First, we compute pairwise cross-correlations within a 5 s sliding window across the continuous data of all five sensors of each array type. Time windows exceeding correlation thresholds of 0.4 for infrasound and 0.45 for seismic are marked as detection windows. A seismic or infrasound detection cluster is then defined as a grouping of at least five detection windows separated by a minimum gap of 3 s. Finally, if a seismic and an infrasound detection cluster overlap, they are merged into a seismo-acoustic event that covers the total duration of both detection clusters. The event detector thresholds were determined by testing a range of values and selecting those that captured most avalanche events while minimizing the total number of seismo-acoustic events.

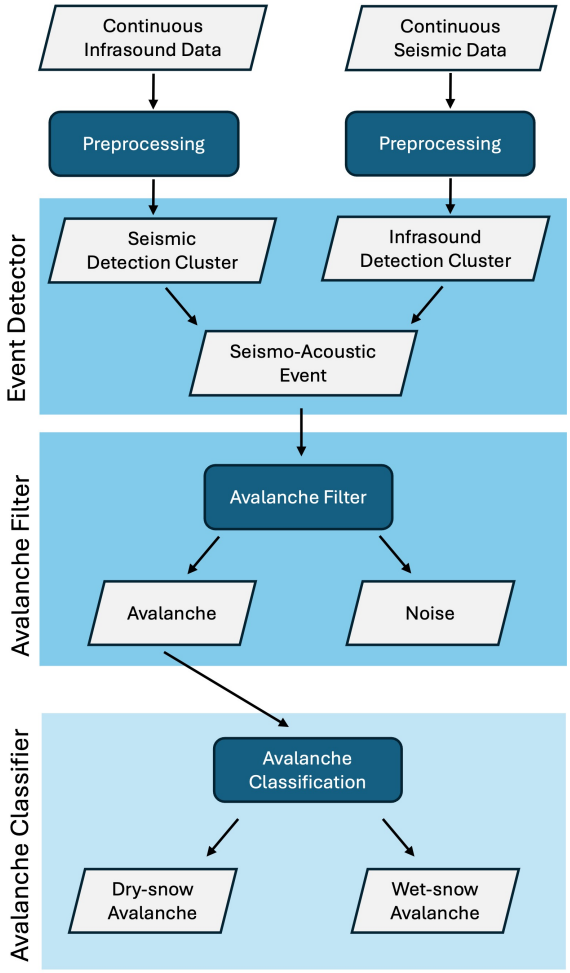


Figure 3: Overview of our seismo-acoustic detection and characterization workflow. Following preprocessing, detection is carried out in two steps: event detection and avalanche filtering. Finally, avalanche classification can be applied as a post-processing step.

The second step, avalanche filtering, aims to remove all non-avalanche events by applying a sequence of threshold-based filter criteria. These filters rely on signal characteristics, such as peak seismic amplitude and signal duration, as well as beamforming-derived source parameters, namely apparent velocity and backazimuth. For example, the event duration filter excludes all seismo-acoustic events with durations shorter than 20 s.

The modular structure of the workflow allows easy adaptation of existing processing steps and thresholds, as well as simple integration of new modules across both processing stages, event detection

and avalanche filtering. Furthermore, it enables custom preprocessing for each avalanche filter, such as specific bandpass-filter settings or specific beamforming parameters. Additionally, avalanche filters can be ordered by their computational efficiency to minimize the computation time.

3.2. Avalanche Characterization

Following avalanche detection, seismo-acoustic data can be used in a post-processing step for avalanche characterization (Figure 3). Here, we introduce a classifier that distinguishes dry- from wet-snow avalanches based on cross-correlations between co-located seismic and infrasound sensors. Following Seupel et al. (2026), these cross-correlations are computed using sliding 5 s windows with 95% overlap and averaged across sensor pairs, suppressing random noise and highlighting coherent seismo-acoustic coupling across the array. Thereafter, the maximum correlation for each avalanche window and its corresponding time lag are determined. Finally, we apply a simple correlation threshold to classify the events: values above the threshold indicate dry-snow avalanches, while those at or below it correspond to wet-snow avalanches. Avalanche classification was applied to the 87 avalanches in our development dataset.

4. RESULTS AND DISCUSSION

4.1. Avalanche Detection

In the following, we evaluate the performance of the detection workflow at its current stage of development. The event detector identified 5,329 seismo-acoustic events, missing only two avalanches (two false negatives (FN)) over the three winter seasons. To reduce the number of false positives (FP), defined as all non-avalanche seismo-acoustic events, a sequence of avalanche filters was applied as a second step. First, we applied an event duration filter, retaining only seismo-acoustic events lasting ≥ 20 s. This computationally fast filter reduces the number of FPs to 3,453 while keeping all avalanche detections (true positives (TP)) identified by the event detector.

In the following, the operation of avalanche filtering is exemplified by the maximum amplitude and mean backazimuth filters. Both are applied to the seismo-acoustic events after duration filtering. Figure 4 shows the relationship between maximum seismic and infrasound amplitudes for the seismo-acoustic detections.

Implementing a seismic maximum amplitude threshold of > 0.05 μm/s (blue dashed line in Figure 4) eliminates 1,318 FPs without missing any avalanche event. For comparison, applying the maximum amplitude infrasound threshold of > 0.1 Pa that was used in the workflow of Belli et al. (2025) (the gray dashed line in Figure 4) would miss 20 of the 87 avalanches in our dataset. This highlights the benefit of adding seismic data. It enables a simple, computationally efficient amplitude filter without excluding mostly wet-snow avalanches, which could be missed by infrasound-only approaches (Mayer et al. 2020).

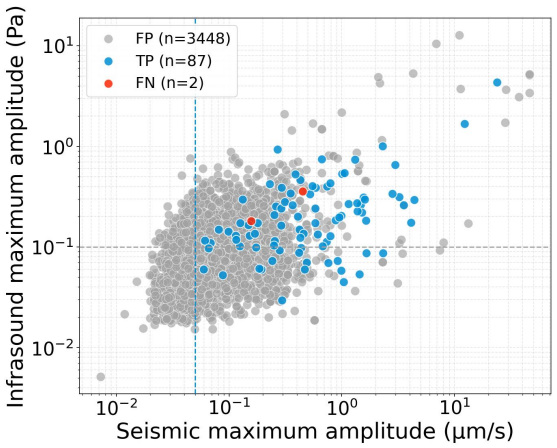


Figure 4: Scatter plot showing the maximum seismic amplitude versus the maximum infrasound amplitude. The blue dashed line indicates the maximum seismic amplitude threshold used in our workflow, the gray dashed line indicates the maximum infrasound amplitude value used in the approach of Belli et al. (2025).

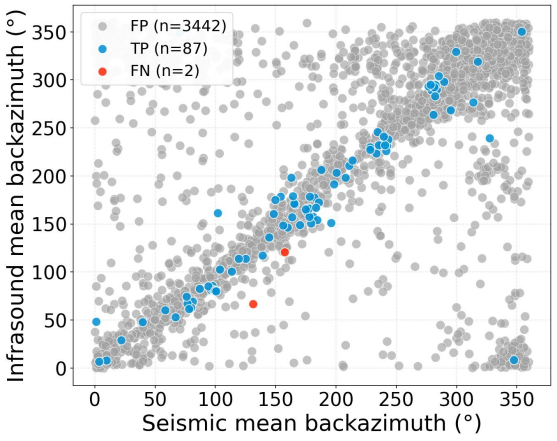


Figure 5: Scatter plot showing the mean backazimuth of seismic data versus the mean backazimuth of infrasound data.

Figure 5 compares the mean backazimuth of seismic and infrasound data, which should be closely aligned for avalanche signals due to sensor co-

location and signal originating from the same source. The observed spread of up to $90.0°$ can be explained by greater scattering in the seismic beamforming results than in the infrasound ones (Seupel et al. 2026). Nevertheless, a filter that allows a maximum difference of $90.0°$ between seismic and infrasound backazimuth still eliminates 434 FPs since several noise events exhibit even larger backazimuth discrepancies.

Using the full set of filters implemented to date, the detection workflow reduces the number of FPs to 356 while keeping the number of missed avalanches (FNs) low (only four avalanches) across the three winters. Although these findings are preliminary, they demonstrate the strong potential of the approach, particularly considering that the development and optimization of the detection workflow is still ongoing.

4.2. Avalanche Characterization

The development of the avalanche type classifier is based on the fact that different avalanche types exhibit distinct seismo-acoustic characteristics as their source processes differ. Infrasound generation is strongly influenced by the presence and extent of the suspension layer (Marchetti, van Herwijnen, et al. 2020; Sovilla et al. 2025; Seupel et al. 2026). Seismic signals are mostly driven by the flowing part of the avalanche (Vilajosana et al. 2007; Pérez-Guillén et al. 2016), however, they can also be significantly affected by the infrasound source (the suspension layer) through seismic-acoustic coupling. This coupling can be visualized by cross-correlating co-located seismic and infrasound sensors. Seupel et al. (2026) showed that for three avalanches released within the same avalanche path, only the dry-snow avalanche exhibited high cross-correlation values, whereas the wet-snow avalanches showed weak correlations.

Based on these observations, we developed an avalanche-type classifier using correlation threshold optimization. The threshold was determined by maximizing the number of correctly classified avalanches, resulting in an optimal value of 0.38. Avalanches with correlations above the threshold are classified as dry-snow, whereas those at or below it as wet-snow. The classification results are shown in Table 1. The results of this simple classification are promising, since only 3 dry-snow avalanches and 6 wet-snow avalanches were misclassified. By definition, there can be no incorrect classifications in the “mixed” class, since that class allows for both types of avalanches.

Table 1: Avalanche classification results evaluated against SNOWPACK-simulated ground truth.

Avalanche Class	***Ground Truth***	***Correct***	***Misclassified***
dry-snow	31	28	3
wet-snow	52	46	6
mixed class	6	14	0

5. CONCLUSIONS AND OUTLOOK

We developed a threshold-based avalanche detection workflow that combines seismic and infrasound array data. Preliminary results show that the complementary information from both sensor types can substantially reduce FPs while retaining most avalanche events. In particular, seismic information helps detect wet-snow avalanches that may not exceed commonly used infrasound amplitude thresholds. Furthermore, a separate post-processing step based on cross-correlations between co-located seismic and infrasound sensors provides additional information on avalanche type. A simple correlation threshold already showed promising discrimination between dry- and wet-snow avalanches, demonstrating the potential of the combined sensor setup not only for avalanche detection but also for subsequent characterization.

Future work will focus on optimizing and evaluating the detection workflow. To reduce the FP rate, we aim to, e.g., integrate additional modules into both the event detector and the avalanche filter stage, a capability facilitated by the workflow’s modular architecture. Furthermore, we plan to evaluate the transferability of our approach at the Vallée de la Sionne test site. Finally, future post-processing developments will explore how seismo-acoustic observations can provide more detailed insights into avalanche characteristics.

ACKNOWLEDGEMENTS

This work was supported by Innosuisse - the Swiss Innovation Agency (grant 37619.1 IP-ENG). We thank Geoprevent, especially Lino Schmid and Johannes Gassner, for sharing the radar data and providing insightful feedback. We also thank numerous colleagues from SLF for their essential help with fieldwork and instrument maintenance.

REFERENCES

Bartelt, P. and Lehning, M. (Nov. 2002). A physical SNOWPACK model for the Swiss avalanche warning. In: Cold Regions Science and Technology 35 (3), pp. 123–145. ISSN: 0165232X. https://doi.org/10.1016/S0165-232X(02)00074-5.

Belli, G., Gheri, D., Bovet, E., Durand, N., Dellavedova, P., and Marchetti, E. (Sept. 2025). Decennial infrasonic array analysis of snow-avalanche activity in Aosta Valley: New perspectives for supporting avalanche forecasting. In: Cold Regions Science and Technology 237, p. 104521. ISSN: 0165-232X. https://doi.org/10.1016/J.COLDREGIONS.2025.104521.

Chen, D., Dreier, L., Steinkogler, W., Vezzosi, S., Magnan, D., and Ulivieri, G. (2024). "Comparative Review of Infrasound Avalanche Detection Algorithms in Operational Applications, Glacier National Park, British Columbia, Canada". In: Proceedings of the International Snow Science Workshop (ISSW 2024), Tromsø, Norway, pp. 1119–1126.

Heck, M., Hobiger, M., Van Herwijnen, A., Schweizer, J., and Fäh, D. (2018). Localization of seismic events produced by avalanches using multiple signal classification. In: Geophysical Journal International 216.1, pp. 201–217.

Johnson, J. B., Anderson, J. F., Marshall, H. P., Havens, S., and Watson, L. M. (Mar. 2021). Snow Avalanche Detection and Source Constraints Made Using a Networked Array of Infrasound Sensors. In: Journal of Geophysical Research: Earth Surface 126 (3). ISSN: 21699011. https://doi.org/10.1029/2020JF005741.

Kogelnig, A., Suriñach, E., Vilajosana, I., Hübl, J., Sovilla, B., Hiller, M., and Dufour, F. (Aug. 2011). On the complementariness of infrasound and seismic sensors for monitoring snow avalanches. In: Natural Hazards and Earth System Sciences 11 (8), pp. 2355–2370. ISSN: 1684-9981. https://doi.org/10.5194/nhess-11-2355-2011.

Lehning, M., Bartelt, P., Brown, B., Fierz, C., and Satyawali, P. (Nov. 2002). A physical SNOWPACK model for the Swiss avalanche warning. In: Cold Regions Science and Technology 35 (3), pp. 147–167. ISSN: 0165232X. https://doi.org/10.1016/S0165-232X(02)00073-3.

Marchetti, E., Ripepe, M., Ulivieri, G., and Kogelnig, A. (Nov. 2015). Infrasound array criteria for automatic detection and front velocity estimation of snow avalanches: Towards a real-time early-warning system. In: Natural Hazards and Earth System Sciences 15 (11), pp. 2545–2555. ISSN: 16849981. https://doi.org/10.5194/nhess-15-2545-2015.

Marchetti, E., van Herwijnen, A., Christen, M., Silengo, M. C., and Barfucci, G. (June 2020). Seismo-acoustic energy partitioning of a powder snow avalanche. In: Earth Surface Dynamics 8 (2), pp. 399–411. ISSN: 2196632X. https://doi.org/10.5194/esurf-8-399-2020.

Mayer, S., Herwijnen, A. van, Ulivieri, G., and Schweizer, J. (May 2020). Evaluating the performance of an operational infrasound avalanche detection system at three locations in the Swiss Alps during two winter seasons. In: Cold Regions Science and Technology 173, p. 102962. ISSN: 0165-232X. https://doi.org/10.1016/J.COLDREGIONS.2019.102962.

Pérez-Guillén, C., Sovilla, B., Suriñach, E., Tapia, M., and Köhler, A. (Jan. 2016). Deducing avalanche size and flow regimes from seismic measurements. In: Cold Regions Science and Technology 121, pp. 25–41. ISSN: 0165232X. https://doi.org/10.1016/j.coldregions.2015.10.004.

Rost, S. and Thomas, C. (Sept. 2002). ARRAY SEISMOLOGY: METHODS AND APPLICATIONS. In: Reviews of Geophysics 40 (3), pp. 2-1-2–27. ISSN: 87551209. https://doi.org/10.1029/2000RG000100.

Schippkus, S. (Aug. 2025). schipp/fast_beamforming: 2025-08-25 update (Version v2). Software. Version v2. https://doi.org/10.5281/zenodo.16939197.

Seupel, C., Pérez-Guillén, C., Fichtner, A., and Herwijnen, A. van (July 2026). Seismo-Acoustic Characterization and Array Processing of Dry- and Wet-Snow Avalanches. In: Journal of Geophysical Research: Earth Surface 131 (7). ISSN: 2169-9003. https://doi.org/10.1029/2025JF008947.

Simeon, A., Pérez-Guillén, C., Volpi, M., Seupel, C., and Herwijnen, A. van (Nov. 2025). Autoencoder-based feature extraction for the automatic detection of snow avalanches in seismic data. In: Geoscientific Model Development 18 (22), pp. 8751–8776. ISSN: 1991-9603. https://doi.org/10.5194/gmd-18-8751-2025.

Sovilla, B., Marchetti, E., Kyburz, M., Köhler, A., Huguenin, P., Calic, I., Kohler, M., Suriñach, E., and Pérez-Guillén, C. (2025). The Dominant source mechanism of infrasound generation in powder snow avalanches. In: Geophysical Research Letters 52.2, e2024GL112886. https://doi.org/10.1029/2024GL112886.

Steinkogler, W., Meier, L., Langeland, S., and Wyssen, ; S. (2016). Avalanche detection systems: A state-of-the art overview on selected operational radar and infrasound systems. In: INTERVENTION, RECOVERY) 1 Wyssen Avalanche Control.

Vilajosana, I., Suriñach, E., Khazaradze, G., and Gauer, P. (Nov. 2007). Snow avalanche energy estimation from seismic signal analysis. In: Cold Regions Science and Technology 50 (1-3), pp. 72–85. ISSN: 0165232X. https://doi.org/10.1016/j.coldregions.2007.03.007.